




Article

# Reaction of Non-Symmetric Schiff Base Metallo-Ligand Complexes Possessing an Oxime Function with Ln Ions

Jean-Pierre Costes <sup>1,2,\*</sup> , Françoise Dahan <sup>1,2</sup>, Arnaud Dupuis <sup>1,2</sup>, Sergiu Shova <sup>3</sup> and Javier Garcia Tojal <sup>4</sup>

<sup>1</sup> Laboratoire de Chimie de Coordination du CNRS, 205, route de Narbonne, BP 44099, Toulouse CEDEX 4 F-31077, France; arnaud.dupuis@gmail.com

<sup>2</sup> Université de Toulouse, UPS, INPT, Toulouse CEDEX 4 F-31077, France

<sup>3</sup> Petru Poni, Institute of Macromolecular Chemistry, Aleea Grigore Ghica Voda 41A, Iasi 700487, Romania; shova@icmpp.ro

<sup>4</sup> Departamento de Química, Facultad de Ciencias, Universidad de Burgos, Plaza Misael Bañuelos s/n, Burgos 09001, Spain; qipgatoj@ubu.es

\* Correspondence: jean-pierre.costes@lcc-toulouse.fr; Tel.: +33-056-133-3100

Received: 29 January 2018; Accepted: 23 February 2018; Published: 9 March 2018

**Abstract:** The preparation of non-symmetric Schiff base ligands possessing one oxime function that is associated to a second function such as pyrrole or phenol function is first described. These ligands, which possess inner N4 or N3O coordination sites, allow formation of cationic or neutral non-symmetric Cu<sup>II</sup> or Ni<sup>II</sup> metallo-ligand complexes under their mono- or di-deprotonated forms. In presence of Lanthanide ions the neutral complexes do not coordinate to the Ln<sup>III</sup> ions, the oxygen atom of the oxime function being only hydrogen-bonded to a water molecule that is linked to the Ln<sup>III</sup> ion. This surprising behavior allows for the isolation of Ln<sup>III</sup> ions by non-interacting metal complexes. Reaction of cationic Ni<sup>II</sup> complexes possessing a protonated oxime function with Ln<sup>III</sup> ions leads to the formation of original and dianionic (Gd(NO<sub>3</sub>)<sub>5</sub>)<sup>2-</sup> entities that are well separated from each other. This work highlights the preparation of well isolated mononuclear Ln<sup>III</sup> entities into a matrix of diamagnetic metal complexes. These new complexes complete our previous work dealing with the complexing ability of the oxime function toward Lanthanide ions. It could open the way to the synthesis of new entities with interesting properties, such as single-ion magnets for example.

**Keywords:** non-symmetric Schiff bases; synthesis; oxime function; 3d–4f complexes; structural determinations

## 1. Introduction

Heterodinuclear complexes associating two different transition metal ions or a transition metal ion with a Lanthanide ion such as Gadolinium are useful in magnetochemistry in order to understand the mechanism of magnetic interactions [1,2]. Their interest is not limited to this research area and, in view of recent reviews, it is clear that they also play a prominent role in catalysis [3,4]. A lot of these heterodinuclear complexes are prepared with use of symmetrical or non-symmetrical Schiff base ligands possessing two coordination sites characterized by different ion affinities and allowing insertion of these ions in a stepwise process without scrambling. H<sub>2</sub>Salen, resulting from condensation of diaminoethane, a diamine synthon, with salicylaldehyde, is a typical Schiff base ligand that is known for long [5]. Such a ligand, being able to coordinate a lot of metal ions, was largely used in coordination chemistry. These complexes and equivalent ones were regularly reviewed [6–9], as more recently those involving ortho-vanillin as ligand [10]. The reactivities of the two amine functions yielding these symmetrical ligands are quite similar, so that the preparation of non-symmetric Schiff

base ligands is not straightforward and necessitates at least one supplementary step [11]. In a first step, one among the two diamine functions must react and the resulting compound, often called half-unit, has to be isolated in good yield. There are several possibilities to prepare these half-units. For a coordination chemist, the template effect making use of a metal ion to isolate the half-unit, is a convenient solution [12,13]. In some cases, a pure organic half-unit can be isolated. This was observed in the reaction of a diketone such as acetylacetone with 1,2 diaminoethane, that gives a half-unit leaving free the second primary diamine function [14,15] or with less reactive amine functions, as in the case of orthophenylenediamine [11,16]. The reaction of butanedione monoxime with several diamines yields organic compounds that correspond to a cyclic aminal in the solid state while an equilibrium between the cyclic form and an open chain structure is evidenced in solution [17]. This open form can then react with a new aldehyde reagent to give a non-symmetric Schiff base ligand able to coordinate a metal ion. In the present paper, we want to show a few examples of non-symmetric Schiff base complexes containing the oxime function that is associated to another function and then check if they are able to coordinate Ln ions according to the “complex as ligand process”. Contrary to metallocrowns made of repeat (M–N–O)<sub>n</sub> units in a cyclic arrangement, which were discovered and developed by Prof. Pecoraro [18,19], our aim is directed toward the syntheses of metal complexes implying an unique –N–O– bridge between the 3d and 4f metal ions. Structural determinations of the starting 3d and the resulting 3d–4f complexes have been helpful to bring the key responses in this study.

## 2. Results and Discussion

The free unsymmetrical Schiff base H<sub>2</sub>L<sup>1</sup> and H<sub>2</sub>L<sup>2</sup> ligands can be prepared by reacting equimolar amounts of 1-(2,4,4-trimethyl-2-imidazolidinyl)-1-ethanone oxime and 1-(2,5,5-trimethylhexahydro-2-pyrimidinyl)-1-ethanone oxime with pyrrole-2-carboxaldehyde in methanol. These ligands are easily characterized by <sup>1</sup>H NMR with presence of signals coming from the oxime and pyrrole moieties and by non-equivalence of the CH<sub>2</sub> signals of the diamino chain in H<sub>2</sub>L<sup>2</sup>. The complexes possessing the protonated oxime function are obtained by the addition of metal perchlorate to the ligands in a methanol solution without addition of base, while those with deprotonated oxime functions are prepared in acetone with triethylamine as a base. These complexes can also be isolated in methanol, but a strong base as NaOH is needed. Eventually, reaction of these diverse Ni or Cu complexes with lanthanide salts in acetone yield new entities for which X-ray structural determinations have been of prime interest to obtain their full characterization.

### 2.1. Structural Characterisation

The results of X-ray diffraction study for NiL<sup>1</sup> complex (**1**) is shown in Figure 1, with relevant bond lengths and angles collected in the Figure caption. It crystallizes in the triclinic *P*-1 space group with two discrete chemically equivalent but crystallographic independent molecules in the unit cell (denoted as **A** and **B**). The central five-membered ring involving the diamine moiety is in the λ gauche conformation for molecule **A** and in the δ gauche conformation for molecule **B**. The Ni<sup>II</sup> ion, surrounded by three five-membered cycles, exhibits a square planar coordination provided by four nitrogen atoms of the tetradentate ligand L<sup>1</sup>. In both asymmetric NiL<sup>1</sup> molecules the Ni–N bond lengths are very similar and vary from 1.820(2) to 1.881(2) Å, so that only the geometric parameters for λ molecule are reported in Figure 1. The deprotonated oxygen atom of the oxime function is not involved in the coordination and the N–O bond length (1.292(2) Å) becomes shorter than the adjacent N=C bond length (1.326(3) Å).

According to X-ray crystallography, the (CuL<sup>2</sup>) (**2**) complex crystallizes also in the triclinic *P*-1 space group. Its molecular crystal structure comprises dinuclear neutral entities (Figure 2) and methanol molecules of crystallization in a 1:2 ratio. Compound **2** shows a 5,6,5-chelate ring arrangement around the Cu<sup>II</sup> ion and presents remarkable structural features when compared to compound **1**. The copper ions of the CuL<sup>2</sup> units, still linked to four nitrogen atoms, are now 0.236(2) Å out of the N<sub>4</sub> coordination plane. Moreover, the copper atom is linked in axial position to the

deprotonated oxygen atom of a neighboring oxime function to form a dinuclear ( $\text{CuL}^2$ )<sub>2</sub> species, where the six-atom Cu–N–O–Cu–N–O metal-cycle acts as a bridging fragment. The axial Cu–O bond lengths of 2.335(2) Å are larger than the equatorial Cu–N bonds, varying from 1.961(2) to 1.993(2) Å.

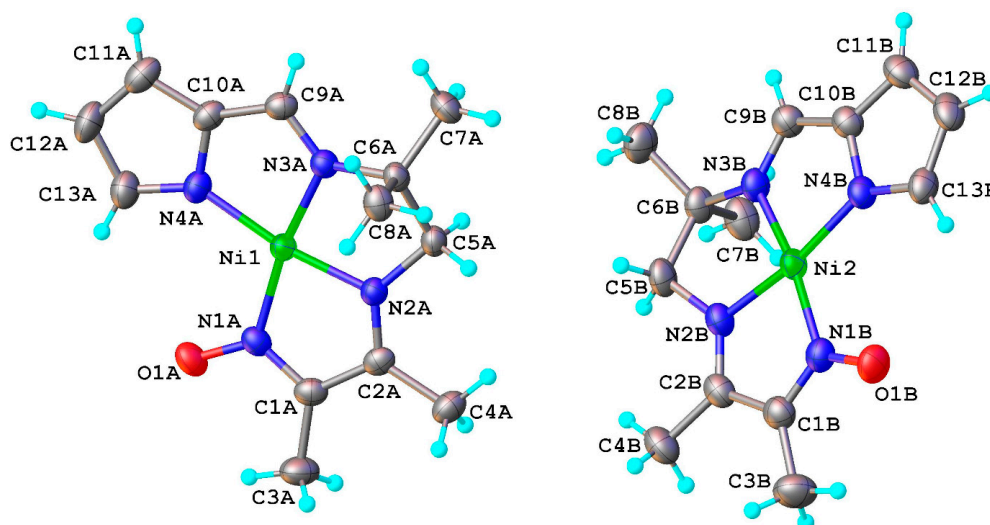


**Figure 1.** View of the asymmetric unit in the crystal structure **1** with atom labeling scheme and thermal ellipsoids at 40% probability level. Selected bond lengths (Å) and angles (°): Ni1–N1A 1.874(2), Ni1–N2A 1.823(2), Ni1–N3A 1.859(2), Ni1–N4A 1.875(2), N1–O1A 1.292(2), N1–C1A 1.326(3); N2A–Ni1–N3A 85.47(8), N2A–Ni1–N1A 84.28(8), N3A–Ni1–N4A 84.64(8), N1A–Ni1–N4A 105.60(9); Ni2–N1B 1.874(2), Ni2–N2B 1.820(2), Ni2–N3B 1.859(2), Ni2–N4B 1.881(2), N1B–O1B 1.282(2), N1B–C1B 1.326(3); N2B–Ni2–N3B 85.27(8), N2B–Ni2–N1B 84.36(9), N3B–Ni2–N4B 84.67(9), N1B–Ni2–N4B 105.72(9).

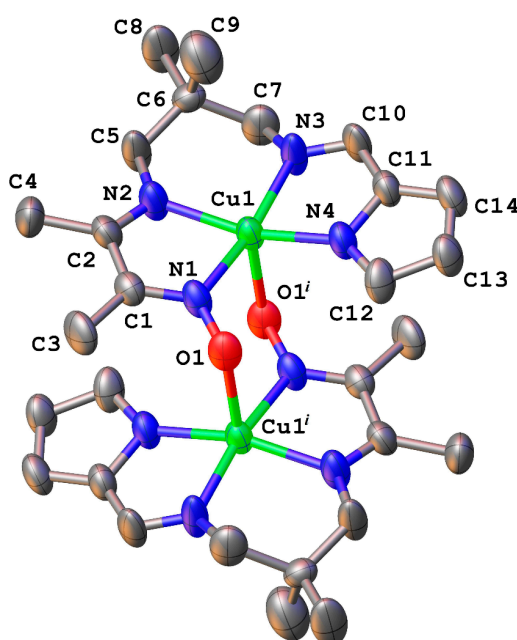


**Figure 2.** X-ray molecular structure of the dinuclear entity in the crystal structure **2** with atom labeling scheme and thermal ellipsoids at 40% probability level. H-atoms are omitted for clarity. Selected bond lengths (Å) and angles (°). Cu–N1 1.971(2), Cu–N2 1.993(2), Cu–N3 1.983(2), Cu–N4 1.961(2), Cu–O1 2.335(2), N1–C1 1.305(3), O1–N1 1.318(3); N1–Cu–N2 80.80(9), N3–Cu–N2 93.19(9), N4–Cu–N3 82.31(9), N4–Cu–N1 100.75(9). Symmetry code: <sup>(i)</sup> 1 – x, 1 – y, 1 – z.

As shown in Figure 3, the asymmetric unit in the crystal structure of **3** includes two chemically identical cationic complexes ( $\text{NiL}^3$ )<sup>+</sup> in a gauche  $\lambda$  conformation, two  $\text{ClO}_4^-$  anions, and one methanol molecule of crystallization. Both of the complexes show the presence of protonated oxime function, the hydrogen atoms being involved as donor atoms in bifurcated hydrogen bonding towards phenoxo, perchlorate (for A) and methanol (for B) oxygen atoms acting as acceptors. In turn, the uncoordinated methanol acts as a donor to form a hydrogen bond with an oxygen atom of the perchlorate ion. Protonation of oxime functions in compound **3** is evidenced by the lengthening of the N–O bond at 1.370(3) Å (for A) and 1.370(3) Å (for B) instead of 1.292(2) and 1.282(2) Å (for compound **2**) and a shortening of the adjacent N=C bond length at 1.291(3) and 1.293(3) Å (for A and B, respectively) instead of 1.326(3) Å (for compound **2**).

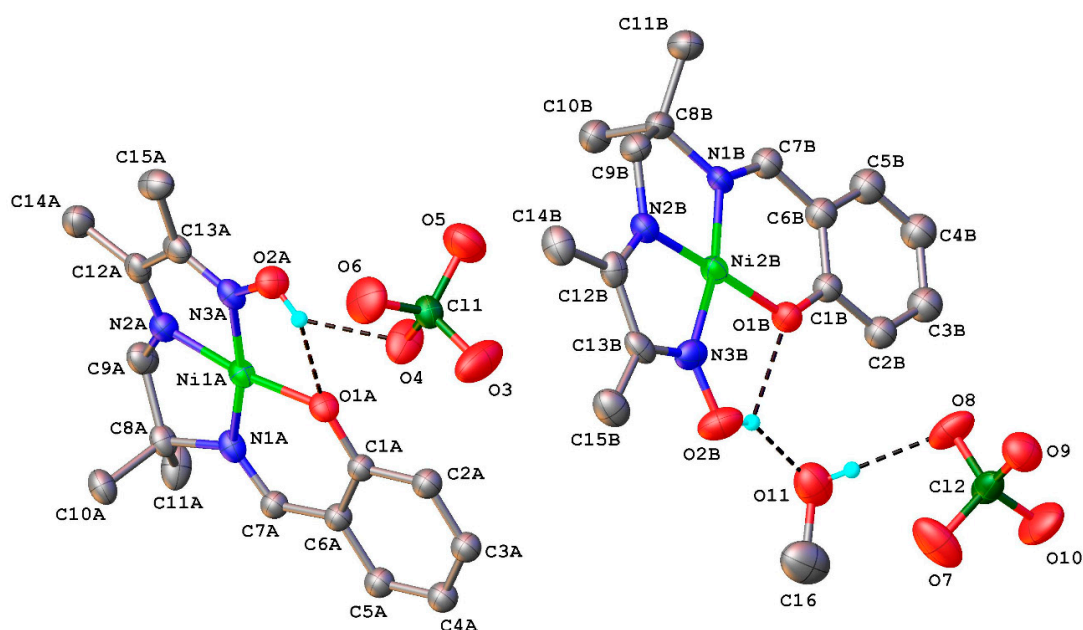


**Figure 3.** View of the asymmetric unit in the crystal structure **3** with atom labelling scheme and thermal ellipsoids at 40% probability level. Non-relevant H-atoms are omitted. Selected bond lengths (Å) and angles (°): Ni1A–O1A 1.7996(17), Ni1A–N2A 1.826(2), Ni1A–N1A 1.828(2), Ni1A–N3A 1.877(2), C13A–N3A 1.291(3), N3A–O2A 1.370(3), Ni2B–O1B 1.8088(17), Ni2B–N2B 1.826(2), Ni2B–N1B 1.829(2), Ni2B–N3B 1.877(2), C13B–N3B 1.293(3), N3B–O2B 1.364(3); O1A–Ni1A–N1A 98.89(8), N2A–Ni1A–N1A 87.10(9), O1A–Ni1A–N3A 92.47(8), N2A–Ni1A–N3A 81.90(9), O1B–Ni2B–N1B 98.46(8), N2B–Ni2B–N1B 86.68(9), O1B–Ni2B–N3B 92.93(9), N2B–Ni2B–N3B 82.11(9). H-bonds parameters: O2A–H···O1A (O2A–H 0.84 Å, H···O1A 2.33 Å, O2A···O1A 2.863(3) Å,  $\angle$ O2A–H–O1A 121.6°); O2A–H···O11 (O2A–H 0.84 Å, H···O11 2.09 Å, O2A···O11 2.778(3) Å,  $\angle$ O2A–H–O11 138.3°); O2B–H···O1B (O2B–H 0.84 Å, H···O1B 2.30 Å, O2B···O1B 2.859(3) Å,  $\angle$ O11–H–O8 124.7°); O11–H···O8 (O11–H 0.84 Å, H···O8 2.03 Å, O11···O8 2.870(3) Å,  $\angle$ O11–H–O8 172.7°).

The crystal structure of compound **5** in the trigonal  $P\bar{3}$  space group is built-up from  $(\text{Er}(\text{NO}_3)_3(\text{H}_2\text{O})_3)$  and  $(\text{CuL}^2)$  neutral entities in 1:3 ratio. An extended asymmetric unit showing the environment of the copper and erbium atoms is depicted in Figure 4. The three nitrato anions and three water molecules define two opposite trihedra having the  $\text{Er}^{\text{III}}$  ion as single vertex, with O–Er–O and N–Er–N angles equal to 80.4(1)° and 99.6(1)°, respectively. The Er–O<sub>water</sub> bond length of 2.325(2) Å is slightly shorter than the Er–O<sub>nitrato</sub> ones of 2.396(2) and 2.404(3) Å. Each water molecule is hydrogen bonded to the oxime oxygen atom of a  $(\text{CuL}^2)$  complex. These  $\text{CuL}^2$  molecules are still associated in dinuclear units through axial Cu–O<sub>oxime</sub> bonds, as in the complex **2**, so that the two  $\text{Er}(\text{NO}_3)_3(\text{H}_2\text{O})_3$  entities hydrogen bonded to a  $(\text{CuL}^2)_2$  unit are positioned in a head-to-tail arrangement, at a distance of 11.515(2) Å. As there are three water molecules in a trihedral arrangement,

we find three  $\text{Er}^{\text{III}}$  ions separated at the same distances from the initial one, with Er–Er–Er angles of  $90.27(2)^\circ$ . The intermolecular hydrogen bonds system induce a two-dimensional arrangement, which determines the formation of supramolecular layers parallel to the 110 plane, as shown in Figure 5. At the same time, the third dimension is limited to the thickness of the  $(\text{CuL}^2)_2$  unit, i.e., the largest distance between the methyl substituents ( $15.854(3) \text{ \AA}$ ) belonging to the two diamino bridges of the  $(\text{CuL}^2)_2$  units. A comparison of dinuclear units in complexes **2** and **5** indicates that hydrogen bonding induces a very slight increase of the N–O bond length in complex **5** ( $1.331(4) \text{ \AA}$  instead of  $1.318(3) \text{ \AA}$  in **2**) along with an equivalent slight decrease of the N=C bond ( $1.290(4)$  against  $1.305(3) \text{ \AA}$  in **2**). But the main difference comes from the axial Cu–O1( $1-x, 1-y, 1-z$ ) bond length, which increases from  $2.335(2) \text{ \AA}$  in **2** to  $2.701(4) \text{ \AA}$  in **5**.

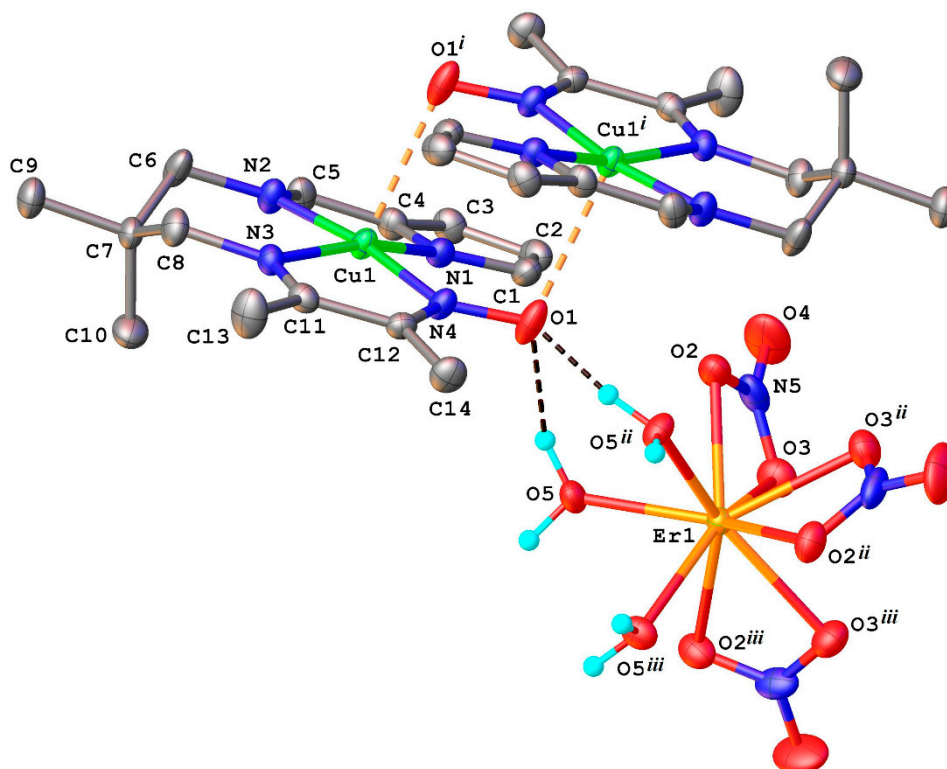


**Figure 4.** Extended asymmetric unit in the crystal structure of **5** and the environment of the copper and erbium atoms with atom labelling scheme and thermal ellipsoids at 40% probability level. Non-relevant H-atoms are omitted. Selected bond lengths ( $\text{\AA}$ ) and angles ( $^\circ$ ): Cu–N1  $1.954(2)$ , Cu–N2  $1.977(2)$ , Cu–N3  $1.995(2)$ , Cu–N4  $1.974(2)$ , Cu–O1  $2.701(4)$ , N4–C12  $1.290(3)$ , O1–N4  $1.331(3)$ , Er–O2  $2.396(2)$ , Er–O3  $2.404(3)$ , Er–O5  $2.325(2)$ ; N1–Cu–N2  $83.0(1)$ , N3–Cu–N2  $92.9(1)$ , N4–Cu–N3  $81.1(1)$ , N4–Cu–N1  $101.6(1)$ . H-bonds parameters: O5–H $\cdots$ O1 (O5–H  $0.92 \text{ \AA}$ , H $\cdots$ O1  $2.29 \text{ \AA}$ , O5 $\cdots$ O1  $3.064(4) \text{ \AA}$ ,  $\angle$ O5–H–O1  $140.7^\circ$ ); Symmetry codes: <sup>(i)</sup>  $1-x, 1-y, 1-z$ ; <sup>(ii)</sup>  $1+y-x, 1-y, z$ ; <sup>(iii)</sup>  $1+y-x, y, z$ .

Complex **6** crystallizes in the triclinic  $P-1$  space group with two cationic  $(\text{NiHL}^5)^+$  and one dianionic  $(\text{Gd}(\text{NO}_3)_5)^{2-}$  entities along with an acetone molecule of crystallization in the unit cell. Three over the five chelating nitrate anions can be considered in an equatorial plane with a practically trigonal arrangement (N–Gd–N angles of  $121.3(1)$ ,  $119.8(1)$ , and  $118.9(1)^\circ$ ), while the two other anions are in an axial position. The Gd–O bond lengths vary from  $2.408(4)$  to  $2.502(4) \text{ \AA}$ , the shortest one being in axial position. Two cationic complexes are needed to compensate the dianionic charge of the  $(\text{Gd}(\text{NO}_3)_5)^{2-}$  entity, so that the charge balance is in agreement with the formation of a  $(\text{NiHL}^5)_2(\text{Gd}(\text{NO}_3)_5)\cdot(\text{CH}_3)_2\text{CO}$  species. The Ni coordination spheres of the two cationic molecules, which exist under their two conformations, are quite similar. As shown in Figure 6, both oxime acts as donor in hydrogen bonding towards nitrate groups (O2–H $\cdots$ O10) and solvate acetone molecule



(O4–H···O20). As expected, the N–O oxime bond lengths (1.372(5) and 1.390(5) Å) are in agreement with protonated oxime functions. The two conformers of each  $(\text{NiHL}^5)^+$  molecule are stacked, with Ni···Ni distances of 3.638(5) Å for the conformers involved in hydrogen bonds and 3.939(5) Å for the other ones. In both cationic complexes, besides the  $\text{N}_3\text{O}$  coordination in equatorial plane, the Ni atoms exhibit short axial contacts with the deprotonated oxygen atom of a neighboring phenoxo function (Ni1–O1(1 – x, 1 – y, 1 – z) 3.243(3) Å and Ni2–O3(–x, –y, –z) 3.343(3) Å), which leads to the formation of dinuclear  $[\text{NiL}^5]_2$  species, as observed in **2** and **5**. Moreover, the Ni2 atom is also axially linked to the oxygen atom of nitrate group at a Ni2–O16 distance of 3.362(4) Å (see Figure 7), indicating that the coordination environment of the Ni atoms are essentially different. They can be characterized as in square-pyramidal 4 + 1 (for Ni1) and octahedral 4 + 2 (for Ni2) coordination geometries. In the crystal, all of the components of the structure are interconnected due to above mentioned interactions to form infinite supramolecular zig-zag chains running along the [111] crystallographic direction, as shown in Figure S1 (see Supplementary Materials).

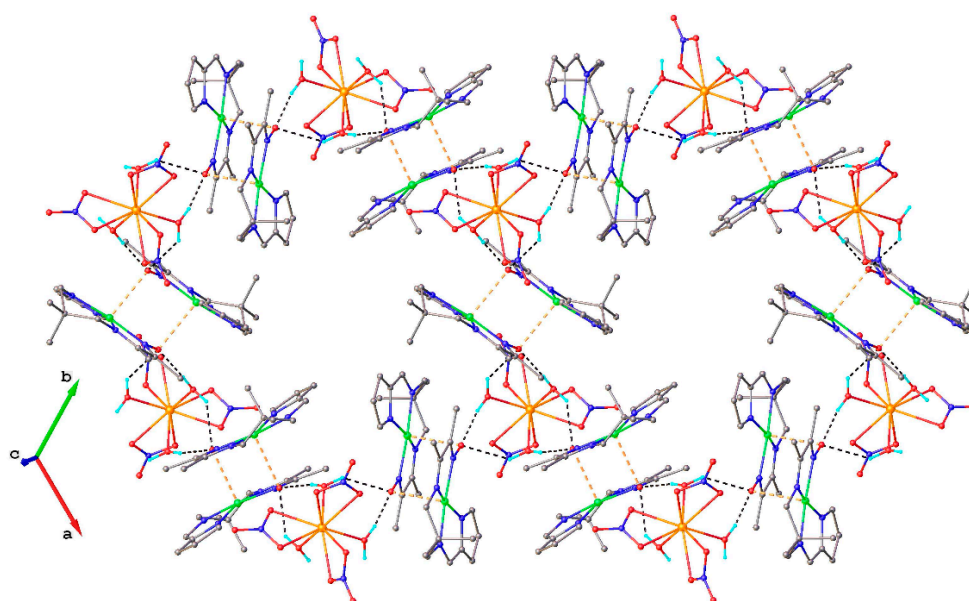


**Figure 5.** View of the two-dimensional network in the crystal structure **5**. H-bonds and the axial Cu–O1(1 – x, 1 – y, 1 – z) bonds are shown in black and orange dashed lines, respectively.

Complexes **7** and **8** are isostructural and crystallize in the monoclinic  $P2_1/n$  space group. The results of X-ray diffraction studies are shown in Figure S2 and Figure 8, respectively. Due to their similarities, only the structure of compound **8** will be reported. The central part of the dinuclear molecular complex  $(\text{CuL}^4 \text{Pr}(\text{NO}_3)_3(\text{H}_2\text{O})_2)$  (**8**) is occupied by the  $\text{Cu}^{\text{II}}$  and  $\text{Pr}^{\text{III}}$  ions connected at 3.6573(9) Å by a double bridge involving phenoxo oxygen and deprotonated oxime functions. The bridging network  $\text{Cu}(\text{O}, \text{N}-\text{O})\text{Pr}$  is not planar, the dihedral angle formed by  $\text{Pr1O1O3}$  and  $\text{Cu1O1N3}$  planar fragments being equal to  $35.4(1)^\circ$ . The  $\text{Cu}^{\text{II}}$  ion has a square-pyramidal environment with an axial water molecule. The  $\text{Pr}^{\text{III}}$  ion is deca-coordinated, surrounded by three oxygen atoms from  $\text{L}^4$  ligand and seven oxygen atoms from three chelating nitrate anions and a water molecule. All of the H-atoms of water molecules act as donor atoms to form several hydrogen bonds, with an intramolecular one involving the water molecules linked to the  $\text{Cu}^{\text{II}}$  and  $\text{Pr}^{\text{III}}$  ions. The remaining intermolecular O–H···O–H bonds along with  $\pi$ – $\pi$  stacking interactions between centro-symmetrically related phenyl rings link the dinuclear complexes into two-dimensional supramolecular layers with packing parallel to [100] plane. A view of this layer is reported on Figure 9.

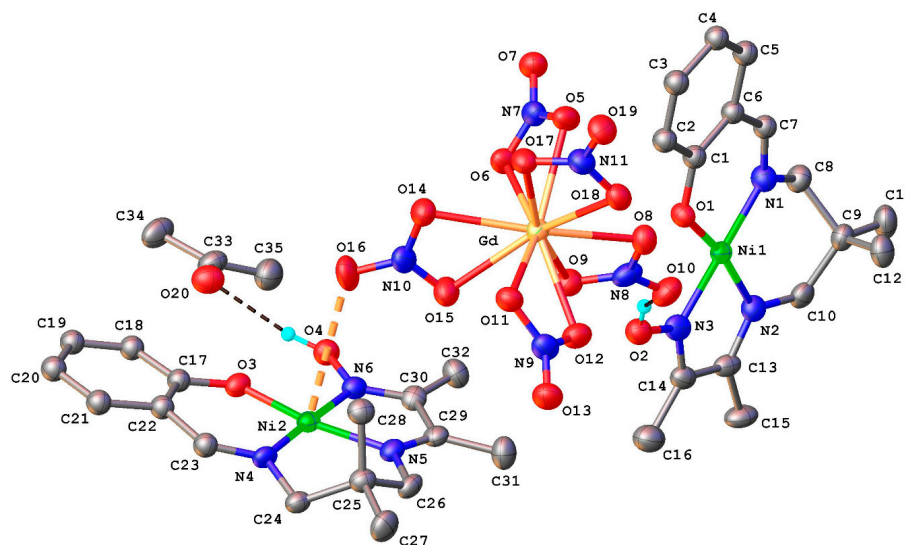


**Figure 6.** Molecular plot for complex **6**, along with selected bond lengths and angles. Hydrogen atoms are omitted for clarity, except those of the two protonated oxime functions. Selected bond lengths (Å) and angles (°): Ni1–O1 1.828(3), Ni1–N1 1.865(4), Ni1–N2 1.886(4), Ni1–N3 1.871(4), N3–O2 1.390(5), C14–N3 1.280(6), Ni2–O3 1.831(3), Ni2–N4 1.858(4), Ni2–N5 1.903(4), Ni2–N6 1.877(4), N6–O4 1.372(5), C30–N6 1.265(6), Gd–O12 2.408(4), Gd–O11 2.478(3), Gd–O5 2.474(3), Gd–O6 2.455(3), Gd–O17 2.486(3), Gd–O18 2.467(3), Gd–O8 2.478(3), Gd–O9 2.502(4), Gd–O15 2.434(3), Gd–O14 2.449(3); O1–Ni1–N1 95.09(16), O1–Ni1–N3 86.53(16), N1–Ni1–N2 97.67(18), N3–Ni1–N2 80.77(18), O3–Ni2–N4 95.32(15), O3–Ni2–N6 86.12(16), N4–Ni2–N5 98.00(17), N6–Ni2–N5 80.57(17). H-bonds parameters: O2–H···O10 (O2–H 0.88 Å, H···O10 2.22 Å, O2···O10 3.023(7) Å, ∠O2–H–O10 151.3°); O2–H···O1 (O2–H 0.88 Å, H···O1 2.24 Å, O2···O1 2.601(7) Å, ∠O2–H–O1 104.3°); O4–H···O20 (O2–H 0.88 Å, H···O20 2.37 Å, O4···O20 3.159(5) Å, ∠O4–H–O20 149.2°); O4–H···O3 (O4–H 0.88 Å, H···O3 2.23 Å, O4···O3 2.595(6) Å, ∠O4–H–O3 101.6°).

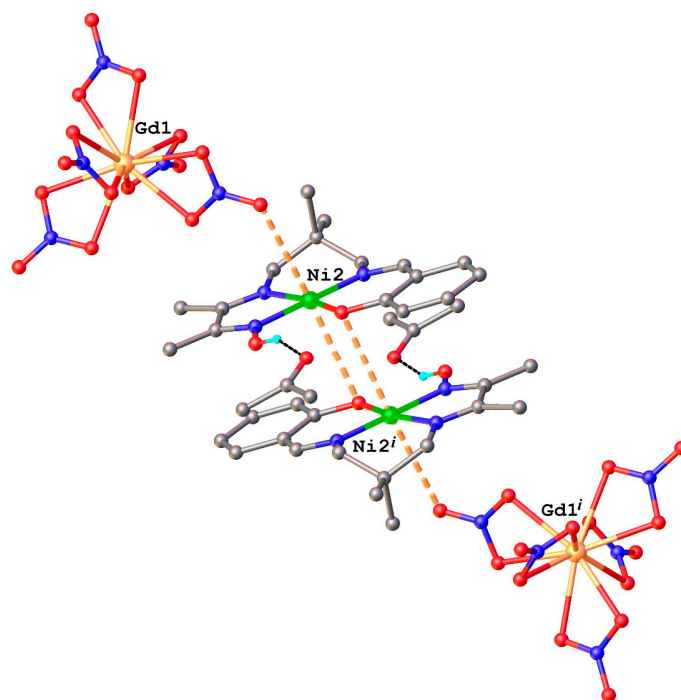


**Figure 7.** View of the  $\{\text{NiL}^5\}_2$  dinuclear entity, showing the Ni2 coordination geometry. Symmetry code:  $^{(i)} 1 - x, 1 - y, 1 - z$ .

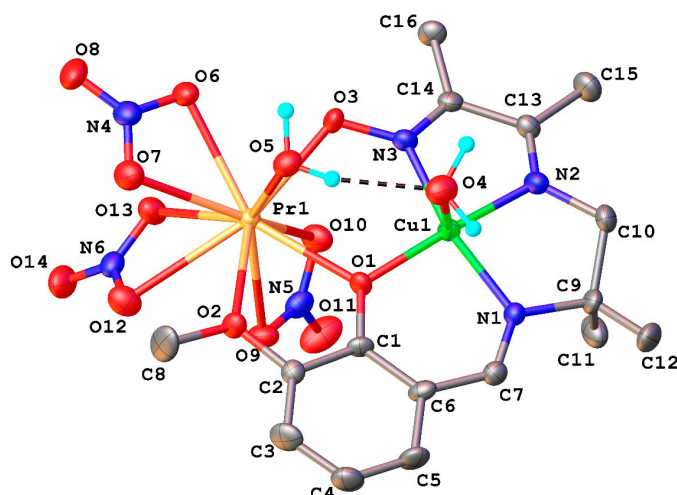


**Figure 8.** X-ray molecular structure of  $\text{CuL}^5 \text{Pr}(\text{NO}_3)_3(\text{H}_2\text{O})_2$  (**8**) with atom labelling scheme and thermal ellipsoids at 40% probability level. Non-relevant H-atoms are omitted. Selected bond lengths ( $\text{\AA}$ ) and angles ( $^\circ$ ). Cu1–N1 1.953(4), Cu1–N2 1.913(5), Cu1–N3 2.014(5), Cu1–O1 1.916(3), Cu1–O4 2.369(5), N3–O3 1.348(5), C14–N3 1.293(5), Pr1–O1 2.449(4), Pr1–O2 2.552(4), Pr1–O3 2.405(4), Pr1–O5 2.549(5), Pr1–O6 2.557(4), Pr1–O7 2.601(5), Pr1–O9 2.640(4), Pr1–O10 2.529(4), Pr1–O12 2.775(5), Pr1–O13 2.547(4); N2–Cu1–N1 83.5(2), O1–Cu1–N1 95.0(2), N2–Cu1–N3 80.1(2), O1–Cu1–N3 99.3(2), Cu1–O1–Pr1 113.2(2), O3–N3–Cu1 125.5(3), N3–O3–Pr1 115.1(3), O3–Pr1–O1 83.4(1). H-bond parameters: O5–H $\cdots$ O4 (O5–H 0.91  $\text{\AA}$ , H $\cdots$ O4 2.01  $\text{\AA}$ , O5 $\cdots$ O4 2.870(7)  $\text{\AA}$ ,  $\angle$ O5–H–O4 156.8 $^\circ$ ).

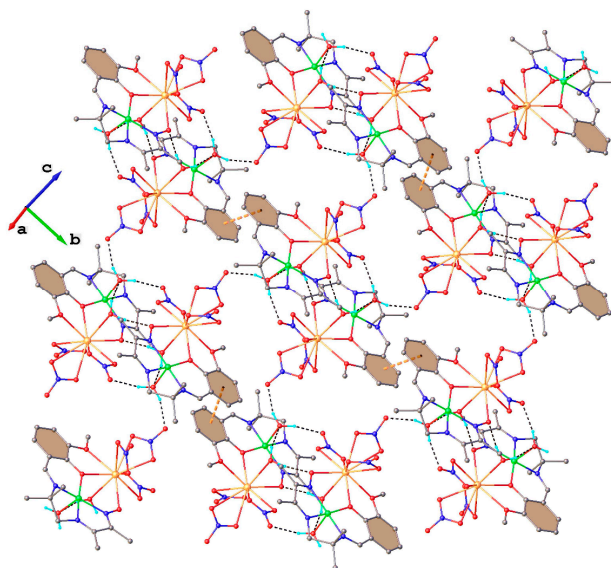


**Figure 9.** View of the 2D supramolecular layer in **8** along  $a$  axis. H-bonds and centroid-to-centroid distances (3.869(5)  $\text{\AA}$ ) are shown in black and orange dashed lines, respectively. H-bond parameters: O5–H $\cdots$ O3 (O5–H 0.91  $\text{\AA}$ , H $\cdots$ O3 2.08  $\text{\AA}$ , O5 $\cdots$ O3(1 -  $x$ , - $y$ , 1 -  $z$ ) 2.974(6)  $\text{\AA}$ ,  $\angle$ O5–H–O3 154.9 $^\circ$ ); O4–H $\cdots$ O14 (O4–H 0.94  $\text{\AA}$ , H $\cdots$ O14 1.90  $\text{\AA}$ , O4 $\cdots$ O14(1 -  $x$ , - $y$ , 1 -  $z$ ) 2.791(8)  $\text{\AA}$ ,  $\angle$ O5–H–O8 158.1 $^\circ$ ).

## 2.2. Magnetic Studies

The magnetic study is limited to copper complexes **2** and **5** and to complex **6**. On the contrary, the magnetic study of complexes **7** and **8** involving phenoxo and oximato bridges, which is much more complex and out of interest here, will not be reported. The magnetic behavior for complex **2** in the form of the thermal variation of the  $\chi_M T$  product ( $\chi_M$  is the molar magnetic susceptibility corrected for the diamagnetism of the ligands) [20] is reported in Figure 10.



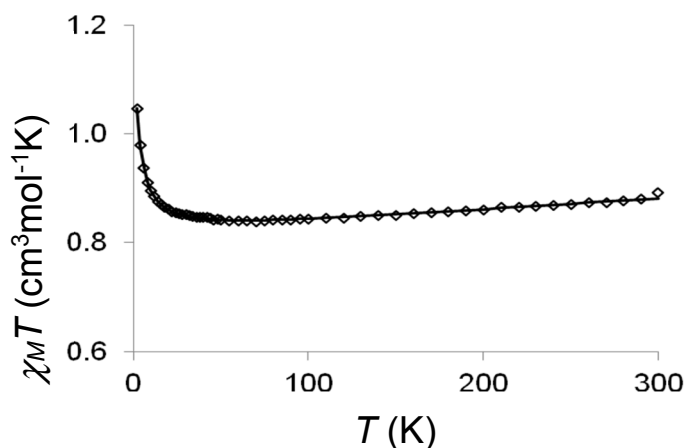


**Figure 10.** Temperature dependence of the  $\chi_M T$  product for complex **2** at an applied magnetic field of 0.1 T. The solid line corresponds to the best data fit (see text).

The  $\chi_M T$  product, which is equal to  $0.89 \text{ cm}^3 \text{ mol}^{-1} \text{ K}$  at 300 K, stays practically constant till 20 K ( $0.80 \text{ cm}^3 \text{ mol}^{-1} \text{ K}$ ), increases smoothly till 2 K ( $1.04 \text{ cm}^3 \text{ mol}^{-1} \text{ K}$ ). The  $\chi_M T$  at room temperature is in the range of the expected value for two isolated  $\text{Cu}^{\text{II}}$  ions. In view of the structure described above, a qualitative analysis was performed with a simple isotropic Hamiltonian  $H = -J(S_{\text{Cu}1} \cdot S_{\text{Cu}2})$ . The resulting ferromagnetic interaction parameter is very weak,  $J_{\text{CuCu}} = 1.56 \text{ cm}^{-1}$ , with  $g = 2.08$  and an agreement factor  $R = \Sigma[(\chi_M T)_{\text{obs}} - (\chi_M T)_{\text{calc}}]^2 / [(\chi_M T)_{\text{obs}}]^2$  equal to  $4 \times 10^{-6}$ . It has to be noted that a weak temperature independent paramagnetism term ( $\text{TIP} = 0.21 \times 10^{-3} \text{ cm}^3 \text{ mol}^{-1}$ ) is needed to fit the high temperature domain of the  $\chi_M T$  curve.

At 300 K, the  $\chi_M T$  product for complex **5** ( $12.7 \text{ cm}^3 \text{ mol}^{-1} \text{ K}$ ) corresponds to the value that is expected for a set of three  $\text{Cu}^{\text{II}}$  and one  $\text{Er}^{\text{III}}$  ions without magnetic interaction ( $12.6 \text{ cm}^3 \text{ mol}^{-1} \text{ K}$ ).

Figure 11 shows that the  $\chi_M T$  product decreases smoothly from 300 to 50 K ( $8.45 \text{ cm}^3 \text{ mol}^{-1} \text{ K}$ ) and then more abruptly to 2 K where it equals  $4.92 \text{ cm}^3 \text{ mol}^{-1} \text{ K}$ . This temperature dependence is attributed to the progressive depopulation of the Erbium excited sublevels. Although the dimeric arrangement of the  $\text{Cu}^{\text{II}}$  ions is still preserved in complex **5**, the structural determination has confirmed an increase of the axial Cu–O oxime bond. Such a structural modification induces a decrease of the ferromagnetic Cu–Cu interaction observed in complex **2**. This interaction, if it is still present, has no visible effect on the experimental  $\chi_M T$  curve, even at 2 K.

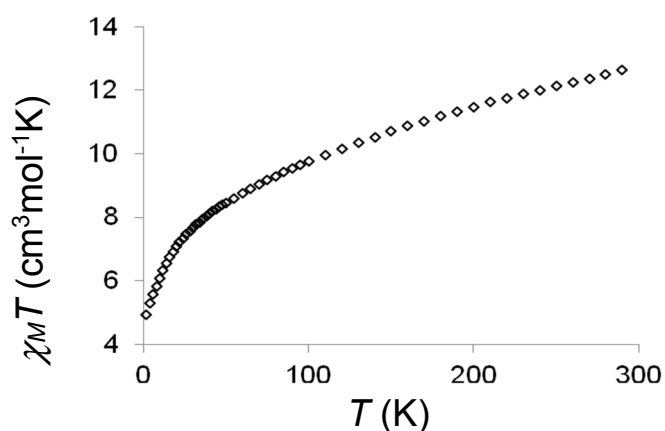


**Figure 11.** Temperature dependence of the  $\chi_M T$  product for complex **5** at an applied magnetic field of 0.1 T.

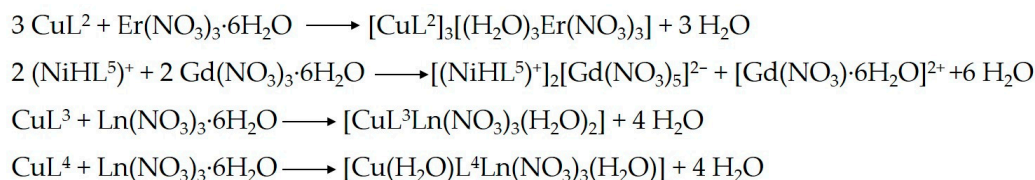
For complex **6**, in which a Gd<sup>III</sup> ion is surrounded by diamagnetic Ni<sup>II</sup> ions, the  $\chi_M T$  product remains constant from 300 to 2 K, with a value around 7.70 cm<sup>3</sup> mol<sup>-1</sup> K, very close from the expected 7.87 cm<sup>3</sup> mol<sup>-1</sup> K value for a non-interacting Gd<sup>III</sup> ion with  $g = 2.0$  (Figure S3).

### 2.3. Discussion

We have previously shown that the half-units resulting from the equimolecular condensation of a diamine with butanedione monoxime adopt in the solid state an aminor structure with a six-membered ring in the chair conformation [17]. In solution, NMR studies demonstrated that a tautomer equilibrium between the cyclic aminor form and an open-chain form is observed. This open form is able to react by its free amine function with organic reagents possessing an aldehyde function, such as pyrrole-2-carboxaldehyde, salicylaldehyde or orthovanillin, in order to yield non-symmetric Schiff base ligands. Further reaction with Ni<sup>II</sup> or Cu<sup>II</sup> ions gives neutral or cationic complexes, depending on the reaction conditions. Working in methanol or ethanol without addition of a base allows isolation of cationic mononuclear complexes such as complexes **3** and **4** in which the oxime function is still protonated. The structural determination of complex **3** confirms presence of a hydrogen atom linked to the oxygen atom of the oxime function along with a perchlorate counter-ion compensating the cationic charge. The use of acetone as solvent in the presence of triethylamine furnishes a neutral complex. The structural determinations of the Ni complex **1** and the Cu complex **2** clearly confirm deprotonation of the oxime function. The deprotonated oxygen atom does not enter into coordination in the case of the four-coordinate square planar Ni complex **1** while it is axially linked to a neighboring Cu<sup>II</sup> ion in **2** to give dinuclear entities, the Cu<sup>II</sup> ion being prone to increase its coordination from four to five, as shown in Figure 2. The involvement of the oximate oxygen atom into coordination or not in complexes **1** and **2** is only due to the preference of Cu<sup>II</sup> ions for pentacoordination and of Ni<sup>II</sup> ions for a square planar environment. The resulting six-membered ring implying two Cu<sup>II</sup> ions and two N–O functions (Cu–N–O–Cu–N–O) is nicely evidenced by the temperature dependence of the magnetic susceptibility. The increase of the  $\chi_M T$  product at low temperature is the result of a weak ferromagnetic interaction between the two Cu ions through the two N–O bridges, as can be expected for a magnetic exchange pathway involving nearly perpendicular magnetic orbitals.

In a following step, complexes **1** and **2** have been used as ligands in order to see if they were able to react with Lanthanide ions. In that case, the oxygen atom of the oxime function is the only one able to link a Ln<sup>III</sup> ion, the pyrrole nitrogen atom coordinated to the Ni<sup>II</sup> or Cu<sup>II</sup> ion being unable to link a supplementary metal ion. The answer is given by the structural determination of complex **5** where we see that each water molecule linked to the Er<sup>III</sup> ion is hydrogen bonded to a deprotonated oxime oxygen atom, but we do not observe a direct link with the Er<sup>III</sup> ion. In the case of complexes **3** and **4**, the oxygen atom able to enter into coordination with a Ln<sup>III</sup> ion is the phenoxo oxygen atom, the oxime oxygen atom being still protonated. Furthermore the (NiHL<sup>5</sup>)<sup>+</sup> complex is cationic, so that it is not surprising to see that the structural determination of complex **6** corresponds to ionic species involving two cationic (NiHL<sup>5</sup>)<sup>+</sup> molecules and the dianionic (Gd(NO<sub>3</sub>)<sub>5</sub>)<sup>2-</sup> entity. In a previous work [21], we published the preparation of the neutral CuL<sup>3</sup> complex in which the oxime function was also deprotonated, the oximate and the phenoxo ones being then able to pick a Ln<sup>III</sup> ion. In the presence of Ln<sup>III</sup> ions, this complex gave new compounds formulated CuL<sup>3</sup>Ln(NO<sub>3</sub>)<sub>3</sub>(H<sub>2</sub>O)<sub>2</sub> (Ln = Er, Yb). Their structural determinations showed that a Cu–N–O–Ln bridge was established. On the contrary, the phenoxo oxygen atom was not involved in the Ln coordination but a supplementary pseudo-bridge implying one oxygen atom of a nitrate anion linked to the Ln<sup>III</sup> and Cu<sup>II</sup> ions according to a  $\eta^2:\eta^1:\mu$  mode was also present (Figure S4). This observation is a little bit surprising if we remember that salen-type complexes can coordinate Ln<sup>III</sup> ions by their two phenoxo oxygen atoms in order to give 3d–4f compounds [22]. Here again, we observe the propensity of Cu<sup>II</sup> ions for pentacoordination. On the contrary, coordination of the phenoxo oxygen atom is exemplified in complexes **7** and **8** in which a methoxy oxygen has been introduced in the vicinity of the phenoxo function. The outer coordination site of the CuL<sup>4</sup> complex is now made of three oxygen atoms that are coordinated to the

$\text{Ln}^{\text{III}}$  ion. According to previous work, it appears that the  $\text{Cu}(\text{H}_2\text{O})\text{L}^4\text{Ln}(\text{NO}_3)_3(\text{H}_2\text{O})$  complexes are isostructural all along the Ln series [23,24]. Eventually the different behaviors of these non-symmetric metallo-ligand complexes in the presence of  $\text{Ln}(\text{NO}_3)_3 \cdot 6\text{H}_2\text{O}$  salts are summarized in the following Scheme 1. Note that the  $\text{NiL}^1$  complex is expected to behave as  $\text{CuL}^2 \cdot \text{CH}_3\text{OH}$ .



**Scheme 1.** Reactions of the different metallo-ligands with  $\text{Ln}(\text{NO}_3)_3 \cdot 6\text{H}_2\text{O}$ .

### 3. Experimental Section

#### 3.1. Materials

The metal salts,  $\text{Ni}(\text{CH}_3\text{COO})_2 \cdot 4\text{H}_2\text{O}$ ,  $\text{Ni}(\text{ClO}_4)_2 \cdot 6\text{H}_2\text{O}$ ,  $\text{Ce}(\text{NO}_3)_3 \cdot 6\text{H}_2\text{O}$ ,  $\text{Pr}(\text{NO}_3)_3 \cdot 6\text{H}_2\text{O}$ ,  $\text{Gd}(\text{NO}_3)_3 \cdot 6\text{H}_2\text{O}$ ,  $\text{Er}(\text{NO}_3)_3 \cdot 6\text{H}_2\text{O}$ , and pyrrole-2-carboxaldehyde, salicylaldehyde (Aldrich, Saint Quentin Fallavier, France) were used as purchased. The syntheses of the starting aiminal ligands, 1-(2,4,4-trimethyl-2-imidazolidinyl)-1-ethanone oxime, 1-(2,5,5-trimethylhexahydro-2pyrimidinyl)-1-ethanone oxime [17] and of the  $\text{CuL}^4 \cdot \text{H}_2\text{O}$  complex [23,24] were previously described. Crystals of  $\text{Cu}(\text{H}_2\text{O})\text{L}^4\text{Ce}(\text{NO}_3)_3(\text{H}_2\text{O})$  (7) and  $\text{Cu}(\text{H}_2\text{O})\text{L}^4\text{Pr}(\text{NO}_3)_3(\text{H}_2\text{O})$  (8) were prepared, as previously described [23,24]. High-grade solvents were used for preparing the different complexes.

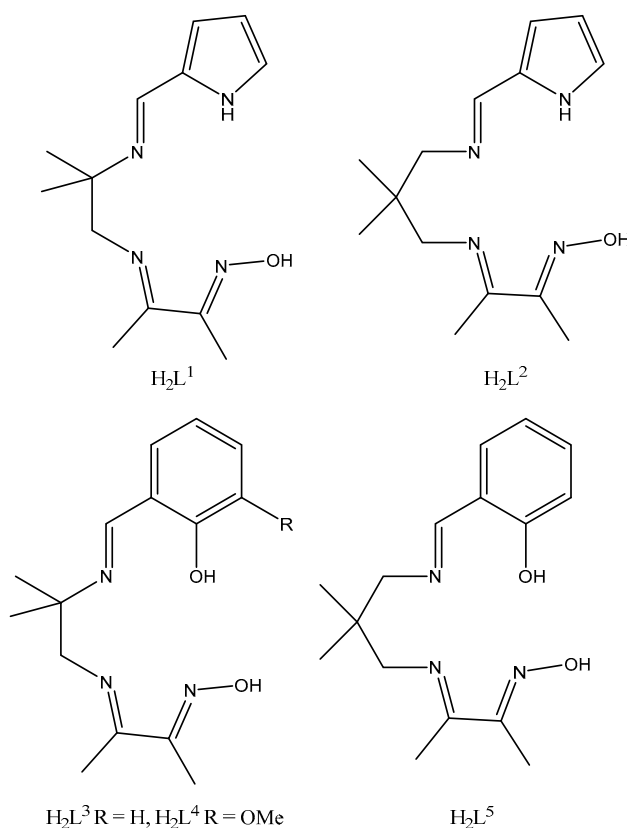
*Caution!* The perchlorate salts of metal complexes with organic ligands are potentially explosive. Although we worked without any incident, their handling, in low amount, necessitates extreme care.

#### 3.2. Ligands

The different non-symmetric  $\text{H}_2\text{L}^1$ ,  $\text{H}_2\text{L}^2$ ,  $\text{H}_2\text{L}^3$ ,  $\text{H}_2\text{L}^4$ ,  $\text{H}_2\text{L}^5$  ligands used in this work are schematized hereunder (Scheme 2). If  $\text{H}_2\text{L}^1$ ,  $\text{H}_2\text{L}^2$  were isolated before complexation, the other ligands were prepared as previously described [23,24].

**$\text{H}_2\text{L}^1$ ,  $\text{H}_2\text{L}^2$  ligands.** A methanol solution (40 mL) of 1-(2,4,4-trimethyl-2-imidazolidinyl)-1-ethanone oxime (1.71 g,  $1 \times 10^{-2}$  mol) or 1-(2,5,5-trimethylhexahydro-2pyrimidinyl)-1-ethanone oxime (1.85 g,  $1 \times 10^{-2}$  mol) and pyrrole-2-carboxaldehyde (0.95 g,  $1 \times 10^{-2}$  mol) was stirred at room temperature for four hours. The resulting precipitate was filtered off and washed with cold methanol. Yield: 40% for  $\text{H}_2\text{L}^1$  and 80% for  $\text{H}_2\text{L}^2$ . Anal. Calcd. for  $\text{H}_2\text{L}^1$ ,  $\text{C}_{13}\text{H}_{20}\text{N}_4\text{O}$  (248.3): C, 62.88; H, 8.12; N, 22.56. Found: C, 62.45; H, 8.05; N, 22.31; for  $\text{H}_2\text{L}^2$ ,  $\text{C}_{14}\text{H}_{22}\text{N}_4\text{O}$  (262.3): C, 64.09; H, 8.45; N, 21.36. Found: C, 63.88; H, 8.38; N, 21.23.  $^1\text{H}$  NMR  $\text{H}_2\text{L}^1$  (400 MHz, 20 °C,  $\text{CDCl}_3$ ):  $\delta$  1.41 (s, 6H,  $(\text{CH}_3)_2\text{C}$ ), 1.96 (s, 3H,  $\text{CH}_3$ ), 2.07 (s, 3H,  $\text{CH}_3$ ), 3.49 (s, 2H,  $\text{CH}_2\text{N}$ ), 6.20 (t,  $J = 2.8$  Hz, 1H,  $\text{C}(3)\text{H}$ ), 6.53 (dd,  $J = 2.8$  and 1.3 Hz, 1H,  $\text{C}(4)\text{H}$ ), 6.81 (l, 1H,  $\text{C}(2)\text{H}$ ), 8.09 (s, 1H,  $\text{CH}$ );  $^{13}\text{C}\{^1\text{H}\}$  NMR (100.63 MHz, 20 °C,  $\text{dmsO } d_6$ ):  $\delta$  9.20 (s,  $\text{CH}_3\text{CNOH}$ ), 13.65 (s,  $\text{CH}_3\text{CN}$ ), 29.32 (s,  $(\text{CH}_3)_2\text{C}$ ), 58.52 (s,  $\text{C}(\text{CH}_3)_2$ ), 70.21 (s,  $\text{CH}_2\text{NC}$ ), 109.05 (s,  $\text{PyrC}(2)\text{H}$ ), 114.12 (s,  $\text{PyrC}(3)$ ), 122.25 (s,  $\text{PyrC}(4)\text{H}$ ), 130.30 (s,  $\text{PyrC}(1)$ ), 152.23 (s,  $\text{HCN}$ ), 156.68 (s,  $\text{CH}_3\text{CNOH}$ ), 163.22 (s,  $\text{CH}_3\text{CN}$ ).

$\text{H}_2\text{L}^2$ : (400 MHz, 20 °C,  $\text{DMSO}-d_6$ ):  $\delta$  1.08 (s, 6H,  $(\text{CH}_3)_2\text{C}$ ), 2.09 (s, 3H,  $\text{CH}_3$ ), 2.10 (s, 3H,  $\text{CH}_3$ ), 3.31 (s, 2H,  $\text{CH}_2\text{N}$ ), 3.51 (s, 2H,  $\text{CH}_2\text{N}$ ), 6.21 (m, 1H,  $\text{C}(3)\text{H}$ ), 6.53 (m, 1H,  $\text{C}(4)\text{H}$ ), 6.97 (m, 1H,  $\text{C}(2)\text{H}$ ), 8.12 (s, 1H,  $\text{CH}$ ), 11.60 (l, 2H,  $\text{NH} + \text{N}-\text{OH}$ );  $^{13}\text{C}\{^1\text{H}\}$  NMR (100.63 MHz, 20 °C,  $\text{dmsO } d_6$ ):  $\delta$  9.14 (s,  $\text{CH}_3\text{CNOH}$ ), 13.34 (s,  $\text{CH}_3\text{CN}$ ), 24.45 (s,  $(\text{CH}_3)_2\text{C}$ ), 36.62 (s,  $\text{C}(\text{CH}_3)_2$ ), 59.66 (s,  $\text{CH}_2\text{NC}$ ), 69.40 (s,  $\text{CH}_2\text{NCH}$ ), 108.91 (s,  $\text{PyrC}(2)\text{H}$ ), 113.21 (s,  $\text{PyrC}(3)$ ), 121.93 (s,  $\text{PyrC}(4)\text{H}$ ), 130.22 (s,  $\text{PyrC}(1)$ ), 152.01 (s,  $\text{HCN}$ ), 156.74 (s,  $\text{CH}_3\text{CNOH}$ ), 163.34 (s,  $\text{CH}_3\text{CN}$ ).



**Scheme 2.** Ligands used in this work.

### 3.3. Complexes

**NiL<sup>1</sup> (1).** Addition of Ni(CH<sub>3</sub>COO)<sub>2</sub>·4H<sub>2</sub>O (0.50 g, 2 mmol) and NaOH (0.16g, 4 mmol) to a stirred solution of H<sub>2</sub>L<sup>1</sup> (0.5 g, 2 mmol) in ethanol (30 mL) gave an orange solution that was heated for 20 min. Cooling induced formation of crystals suitable for XRD. Yield (0.15 g, 50%). Anal. Calcd. for C<sub>13</sub>H<sub>18</sub>N<sub>4</sub>NiO (305.0): C, 51.19; H, 5.95; N, 18.37. Found: C, 49.88; H, 5.81; N, 18.03.

**CuL<sup>2</sup>·CH<sub>3</sub>OH (2).** A mixture of H<sub>2</sub>L<sup>2</sup> (0.52 g, 2 mmol), Cu(ClO<sub>4</sub>)<sub>2</sub>·6H<sub>2</sub>O (0.74 g, 2 mmol) and triethylamine (0.4 g, 4 mmol) in acetone (20 mL) was stirred at room temperature for 1 h. The lilac precipitate which appeared was filtered off, washed with acetone, diethyl ether and dried. Recrystallisation from methanol yielded crystals suitable for XRD. Yield: 0.52 g (73%). Anal. Calcd. for C<sub>14</sub>H<sub>24</sub>CuN<sub>4</sub>O<sub>2</sub> (355.9): C, 50.62; H, 6.80; N, 15.74. Found: C, 50.31; H, 6.58; N, 15.56.

**(NiHL<sup>3</sup>)(ClO<sub>4</sub>)·0.25CH<sub>3</sub>OH (3).** A mixture of H<sub>2</sub>L<sup>3</sup> (0.55 g, 2 mmol), Ni(ClO<sub>4</sub>)<sub>2</sub>·6H<sub>2</sub>O (0.73 g, 2 mmol) in methanol (20 mL) was stirred at room temperature for 1 h. The orange precipitate that appeared was filtered off, washed with cold methanol, diethyl ether and dried. Recrystallisation from methanol yielded crystals suitable for XRD. Yield: 0.54 g (61%). Anal. Calcd. for C<sub>15.25</sub>H<sub>21</sub>ClN<sub>3</sub>NiO<sub>6.25</sub> (440.5): C, 41.58; H, 4.81; N, 9.54. Found: C, 41.08; H, 4.34; N, 9.28.

**(NiHL<sup>5</sup>)(ClO<sub>4</sub>)·CH<sub>3</sub>OH (4).** A mixture of H<sub>2</sub>L<sup>5</sup> (0.58 g, 2 mmol), Ni(ClO<sub>4</sub>)<sub>2</sub>·6H<sub>2</sub>O (0.73 g, 2 mmol) in methanol (20 mL) was stirred at room temperature for 1 h. The orange precipitate that appeared was filtered off, washed with cold methanol, diethyl ether and dried. Yield: 0.60 g (63%). Anal. Calcd. for C<sub>17</sub>H<sub>26</sub>ClN<sub>3</sub>NiO<sub>7</sub> (478.6): C, 42.67; H, 5.48; N, 8.78. Found: C, 42.43; H, 5.30; N, 8.59.

**(CuL<sup>2</sup>)<sub>3</sub>Er(NO<sub>3</sub>)<sub>3</sub>(H<sub>2</sub>O)<sub>3</sub> (5).** A mixture of CuL<sup>2</sup> (0.18 g, 0.5 mmol) and Er(NO<sub>3</sub>)<sub>3</sub>·6H<sub>2</sub>O (0.23 g, 0.5 mmol) in acetone (20 mL) was stirred at room temperature for 1 h. The resulting solution was filtered off and left aside. Crystals suitable for X-ray appeared two days later. Yield: 0.19 g (42%). Anal. Calcd. for C<sub>42</sub>H<sub>66</sub>Cu<sub>3</sub>ErN<sub>15</sub>O<sub>15</sub> (1379.0): C, 36.58; H, 4.82; N, 15.24. Found: C, 36.37; H, 4.65; N, 14.61.

(NiHL<sup>5</sup>)<sub>2</sub>Gd(NO<sub>3</sub>)<sub>5</sub>(CH<sub>3</sub>COCH<sub>3</sub>) (**6**). A mixture of (NiHL<sup>5</sup>)(ClO<sub>4</sub>)·MeOH (0.24 g, 0.5 mmol) and Gd(NO<sub>3</sub>)<sub>3</sub>·5H<sub>2</sub>O (0.22 g, 0.5 mmol) in acetone (20 mL) was stirred at room temperature for 1 h. The resulting orange solution was filtered off and left aside. Crystals suitable for X-ray appeared two days later. Yield: 0.11 g (35%). Anal. Calcd. for C<sub>35</sub>H<sub>50</sub>GdN<sub>11</sub>Ni<sub>2</sub>O<sub>20</sub> (1219.5): C, 34.47; H, 4.13; N, 12.63. Found: C, 34.23; H, 3.98; N, 12.05.

**Physical measurements.** C, H, and N elemental analyses were carried out at the Laboratoire de Chimie de Coordination, Microanalytical department, in Toulouse, France. 1D <sup>1</sup>H and <sup>13</sup>C NMR spectra were acquired at 400.16 MHz (<sup>1</sup>H) or 100.63 MHz (<sup>13</sup>C) on Bruker Avance 400 spectrometer (BRUKER FRANCE, Wissembourg, France) using CDCl<sub>3</sub> or DMSO-*d*<sub>6</sub> as solvent. Chemical shifts are given in ppm versus TMS (<sup>1</sup>H and <sup>13</sup>C). Magnetic data were obtained with a Quantum Design MPMS SQUID susceptometer. All samples were 3 mm diameter pellets molded from ground crystalline samples. Magnetic susceptibility measurements were performed in the 2–300 K temperature range in a 0.1 T applied magnetic field, and diamagnetic corrections were applied by using Pascal's constants [20]. The magnetic susceptibilities have been computed by exact calculations of the energy levels associated to the spin Hamiltonian through diagonalization of the full matrix with a general program for axial symmetry [25]. Least-squares fittings were accomplished with an adapted version of the function-minimization program MINUIT [26].

#### 3.4. Crystallographic Data Collections and Structure Determinations for **1**, **2**, **3**, **5**, **6**, **7**, and **8**

Crystals of **1**, **2**, **3**, **5**, **6**, **7** and **8** were kept in the mother liquor until they were dipped into oil. The chosen crystals were glued on a glass fibre and measured at 293 K, except for (**3**) that quickly cooled down to 160 K. The selected crystals of **1** (red, 0.50 × 0.35 × 0.10 mm<sup>3</sup>), **2** (brown, 0.45 × 0.45 × 0.20 mm<sup>3</sup>), **3** (red, 0.40 × 0.30 × 0.10 mm<sup>3</sup>), **5** (dark-red, 0.50 × 0.35 × 0.10 mm<sup>3</sup>), **6** (red, 0.50 × 0.30 × 0.10 mm<sup>3</sup>), **7** (brown-red, 0.40 × 0.40 × 0.05 mm<sup>3</sup>) and **8** (purple, 0.40 × 0.35 × 0.05 mm<sup>3</sup>) were mounted on an Enraf-Nonius CAD4 or a STOE-IPDS (**3**) diffractometer using a graphite-monochromated Mo K $\alpha$  radiation ( $\lambda = 0.71073 \text{ \AA}$ ) and equipped with an Oxford Instrument Cooler Device. The unit cell determinations were obtained by the least-square fit of the setting angles of 25 reflections in the 12.0–19.5°  $\theta$  range. The reflections were corrected for Lorentz-polarization effects with the MolEN package [27] and semi-empirical absorption corrections based on  $\psi$  scans were applied for the CAD4 measurements [28]. The structures have been solved by Direct Methods using SHELXS97 [29] and refined by means of least-squares procedures on a F<sup>2</sup> with the program SHELXL97 included in the software package WinGX version 1.63 [30]. Atomic Scattering Factors were taken from International tables for X-ray Crystallography [31]. All non-hydrogen atoms were anisotropically refined, and all of the hydrogen atoms were refined by using a riding model. Drawings of molecules are performed with Olex2 program [32]. These data can be obtained free of charge via [www.ccdc.cam.ac.uk/conts/retrieving.html](http://www.ccdc.cam.ac.uk/conts/retrieving.html) (or from the Cambridge Crystallographic Data Centre, 12 Union Road, Cambridge CB2 1EZ, UK; fax: (+44) 1223-336-033; or deposit@ccdc.ca.ac.uk).

**Crystal data for 1.** C<sub>13</sub>H<sub>18</sub>N<sub>4</sub>NiO, M = 305.02, triclinic, *P*–1, Z = 4, *a* = 10.6904(15), *b* = 13.0941(13), *c* = 10.0521(13) Å,  $\alpha = 94.104(9)$ ,  $\beta = 101.815(11)$ ,  $\gamma = 95.942(10)^\circ$ , *V* = 1368.7(3) Å<sup>3</sup>, 5957 collected reflections, 4690 unique reflections, R-factor = 0.0316, weighted R-factor = 0.0784 for 4690 contributing reflections (*I* > 2 $\sigma$  (*I*)) and 343 parameters. CCDC 1820853.

**Crystal data for 2.** C<sub>30</sub>H<sub>48</sub>Cu<sub>2</sub>N<sub>8</sub>O<sub>4</sub>, M = 711.84, triclinic, *P*–1, Z = 1, *a* = 10.0995(8), *b* = 10.1606(14), *c* = 9.0768(10) Å,  $\alpha = 114.210(11)$ ,  $\beta = 91.365(8)$ ,  $\gamma = 94.020(9)^\circ$ , *V* = 846.01(16) Å<sup>3</sup>, 3682 collected reflections, 2905 unique reflections, R-factor = 0.0248, weighted R-factor = 0.0495 for 2905 contributing reflections (*I* > 2 $\sigma$  (*I*)) and 201 parameters. CCDC 1820854.

**Crystal data for 3.** C<sub>15.25</sub>H<sub>21</sub>ClN<sub>3</sub>NiO<sub>6.25</sub>, M = 440.50, triclinic, *P*–1, Z = 4, *a* = 10.6278(15), *b* = 17.806(2), *c* = 9.7465(13) Å,  $\alpha = 96.093(16)$ ,  $\beta = 90.758(17)$ ,  $\gamma = 102.995(16)^\circ$ , *V* = 1785.7(4) Å<sup>3</sup>, 14476 collected reflections, 5334 unique reflections (R<sub>int</sub> = 0.0419), R-factor = 0.0287, weighted R-factor = 0.0587 for 5334 contributing reflections (*I* > 2 $\sigma$  (*I*)) and 456 parameters. CCDC 1820858.



**Crystal data for 5.**  $C_{42}H_{66}Cu_3ErN_{15}O_{15}$ ,  $M = 1378.98$ , trigonal,  $P\bar{3}$ ,  $Z = 2$ ,  $a = 16.320(4)$ ,  $b = 16.320(4)$ ,  $c = 12.476(3)$  Å,  $\alpha = \beta = 90^\circ$ ,  $\gamma = 120^\circ$ ,  $V = 2877.7(12)$  Å<sup>3</sup>, 12,522 collected reflections, 4184 unique reflections ( $R_{int} = 0.0228$ ), R-factor = 0.0277, weighted R-factor = 0.0585 for 3304 contributing reflections ( $I > 2\sigma(I)$ ) and 237 parameters. CCDC 1820855.

**Crystal data for 6.**  $C_{35}H_{50}GdN_{11}Ni_2O_{20}$ ,  $M = 1219.53$ , triclinic,  $P\bar{1}$ ,  $Z = 2$ ,  $a = 13.6209(16)$ ,  $b = 16.9267(18)$ ,  $c = 12.3668(16)$  Å,  $\alpha = 110.594(10)$ ,  $\beta = 111.613(11)$ ,  $\gamma = 70.165(10)^\circ$ ,  $V = 2408.2(5)$  Å<sup>3</sup>, 8458 collected reflections, 5430 unique reflections, R-factor = 0.0303, weighted R-factor = 0.0595 for 5430 contributing reflections ( $I > 2\sigma(I)$ ) and 554 parameters. CCDC 1820859.

**Crystal data for 7.**  $C_{16}H_{25}CeCuN_6O_{14}$ ,  $M = 729.08$ , monoclinic,  $P2_1/n$ ,  $Z = 4$ ,  $a = 12.8286(11)$ ,  $b = 13.6773(11)$ ,  $c = 14.5443(14)$  Å,  $\alpha = \gamma = 90^\circ$ ,  $\beta = 94.543(8)^\circ$ ,  $V = 2543.9(4)$  Å<sup>3</sup>, 4669 collected reflections, 4465 unique reflections ( $R_{int} = 0.0170$ ), R-factor = 0.0267, weighted R-factor = 0.0504 for 3301 contributing reflections ( $I > 2\sigma(I)$ ) and 359 parameters. CCDC 1820851.

**Crystal data for 8.**  $C_{16}H_{25}CuN_6O_{14}Pr$ ,  $M = 729.87$ , monoclinic,  $P2_1/n$ ,  $Z = 4$ ,  $a = 12.7818(16)$ ,  $b = 13.6298(16)$ ,  $c = 14.5042(19)$  Å,  $\alpha = \gamma = 90^\circ$ ,  $\beta = 94.530(17)^\circ$ ,  $V = 2518.9(5)$  Å<sup>3</sup>, 4625 collected reflections, 4423 unique reflections ( $R_{int} = 0.0286$ ), R-factor = 0.0363, weighted R-factor = 0.0867 for 3129 contributing reflections ( $I > 2\sigma(I)$ ) and 359 parameters. CCDC 1820869.

#### 4. Conclusions

In the present paper, we describe the preparation of complexes implying non-symmetric Schiff base ligands possessing an oxime function associated to a second function such as pyrrole or phenol function. These ligands, which possess inner N4 or N3O coordination sites, are able to coordinate Cu<sup>II</sup> or Ni<sup>II</sup> ions under their mono- or di-deprotonated forms. Once deprotonated, the oxygen atom of the oxime function can remain free, as in the case of Ni<sup>II</sup> complexes or enter into coordination with a neighboring Cu<sup>II</sup> ion to yield dinuclear copper complexes possessing a double oximato bridge, which confirms the propensity of Cu<sup>II</sup> ions toward pentacoordination. In a second step, we have a look at the reaction of these complexes with Lanthanide ions. Several behaviors were observed. With a non-deprotonated oxime function, the resulting compound corresponds to an ionic species. This example allowed for the characterization of a surprising dianionic  $(Gd(NO_3)_5)^{2-}$  entity made of five nitrate anions chelating the Gd ion in equatorial position for three of them and in apical position for the last two nitrate ligands. When the deprotonated oxime function is associated to a pyrrole function that is unable to react with a supplementary metal ion, the oximato oxygen atom is hydrogen-bonded to water molecules brought by the Ln ion. If the deprotonated oxime function is associated to a phenol function, the oximato oxygen atom is directly linked to the Ln ion while the phenoxo oxygen atom enters into coordination only if it is surrounded by a supplementary donor atom in its vicinity. Use of these non-symmetrical Schiff base complexes as ligands can yield 3d–4f complexes involving a unique 3d–N–O–4f oximato bridge or a double phenoxo–oximato bridge. This work highlights the preparation of well isolated mononuclear Ln<sup>III</sup> entities into a matrix of diamagnetic metal complexes according to an experimental process making use of non-symmetric Schiff base metallo-ligand complexes. These new complexes complete our previous work dealing with the complexing ability of the oxime function toward Lanthanide ions. It could open the way to the synthesis of new entities with interesting properties, such as single-ion magnets for example.

**Supplementary Materials:** The following are available online at [www.mdpi.com/2304-6740/6/1/33/s1](http://www.mdpi.com/2304-6740/6/1/33/s1), Cif and check cif files of **1**, **2**, **3**, **5**, **6**, **7**, and **8**, Figure S1: Supramolecular chain in the crystal structure **6**, Figure S2: X-ray molecular structure of  $CuL^5Ce(NO_3)_3(H_2O)_2$  (**7**), Figure S3: Temperature dependence of the  $\chi_M T$  product for complex **6** at an applied magnetic field of 0.1 T, Figure S4: Molecular plot for complex  $CuL^5Er(NO_3)_3(H_2O)_2$  [**21**].

**Author Contributions:** Jean-Pierre Costes conceived and designed the experiments; Arnaud Dupuis and Javier Garcia Tojal performed the experiments; Françoise Dahan and Sergiu Shova analyzed the data; Jean-Pierre Costes and Sergiu Shova wrote the paper.

**Conflicts of Interest:** The authors declare no conflict of interest.

## References

1. Kahn, O. *Molecular Magnetism*; VCH: New York, NY, USA, 1993.
2. Benelli, C.; Gatteschi, D. Magnetism of Lanthanides in Molecular Materials with Transition-Metal Ions and Organic Radicals. *Chem. Rev.* **2002**, *102*, 2369–2387. [[CrossRef](#)] [[PubMed](#)]
3. Lorion, M.; Maindan, K.; Kapdi, A.R.; Ackermann, L. Heteromultimetallic catalysis for sustainable organic syntheses. *Chem. Soc. Rev.* **2017**, *46*, 7399–7420. [[CrossRef](#)] [[PubMed](#)]
4. Liu, X.; Manzur, C.; Novoa, N.; Celedón, S.; Carrillo, D.; Hamon, J. Multidentate unsymmetrically-substituted Schiff bases and their metal complexes: Synthesis, functional materials properties, and applications to catalysis. *Coord. Chem. Rev.* **2018**, *357*, 144–172. [[CrossRef](#)]
5. Pfeiffer, P.; Breith, E.; Lülle, E.; Tsumaki, T. Tricyclische orthokondensierte Nebenvalenzringe. *Justus Liebigs Ann. Chem.* **1933**, *503*, 84–130. [[CrossRef](#)]
6. Vigato, P.A.; Tamburini, S. The challenge of cyclic and acyclic Schiff bases and related derivatives. *Coord. Chem. Rev.* **2004**, *248*, 1717–2128. [[CrossRef](#)]
7. Vigato, P.A.; Tamburini, S.; Batolo, L. The development of compartmental macrocyclic Schiff bases and related polyamine derivatives. *Coord. Chem. Rev.* **2007**, *251*, 1311–1492. [[CrossRef](#)]
8. Vigato, P.A.; Tamburini, S. Advances in acyclic compartmental ligands and related complexes. *Coord. Chem. Rev.* **2008**, *252*, 1871–1995. [[CrossRef](#)]
9. Vigato, P.A.; Peruzzo, V.; Tamburini, S. Acyclic and cyclic compartmental ligands: Recent results and perspectives. *Coord. Chem. Rev.* **2012**, *256*, 953–1114. [[CrossRef](#)]
10. Andruh, M. The exceptionally rich coordination chemistry generated by Schiff-base ligands derived from *o*-vanillin. *Dalton Trans.* **2015**, *44*, 16633–16653. [[CrossRef](#)] [[PubMed](#)]
11. Kleij, A.W. Nonsymmetrical Salen Ligands and Their Complexes: Synthesis and Applications. *Eur. J. Inorg. Chem.* **2009**, *2009*, 193–205. [[CrossRef](#)]
12. Costes, J.P.; Chiboub Fellah, F.Z.; Dahan, F.; Duhayon, C. Role of the kinetic template effect in the syntheses of non-symmetric Schiff base complexes. *Polyhedron* **2013**, *52*, 1065–1072. [[CrossRef](#)]
13. Burke, P.J.; McMillin, D.R. Unsymmetrical Ligand Complexes of Cu, Ni, and Co derived from Salicylaldehyde and 1,3-Propanediamine with either Pyridine-2-carbaldehyde or Pyrrole-2-carbaldehyde. *J. Chem. Soc. Dalton* **1980**, 1794–1796. [[CrossRef](#)]
14. Costes, J.P.; Cros, G.; Darbieu, M.H.; Laurent, J.P. The non-template synthesis of novel non-symmetrical, tetradentate Schiff bases. Their nickel(II) and cobalt(III) complexes. *Inorg. Chim. Acta* **1982**, *60*, 111–114. [[CrossRef](#)]
15. Costes, J.P.; Dahan, F.; Laurent, J.P. New route to bimetallic imidazolate-bridged complexes. 6. Structural and magnetic consequences of steric effects in mono and dinuclear nickel(II) and copper(II) complexes involving 4-methylimidazole as ligand. *Inorg. Chem.* **1991**, *30*, 1887–1892. [[CrossRef](#)]
16. Béreau, V.; Dhers, S.; Costes, J.P.; Duhayon, C.; Sutter, J.P. Syntheses, Structures, and Magnetic Properties of Symmetric and Dissymmetric Ester-Functionalized 3d-4f Schiff Base Complexes. *Eur. J. Inorg. Chem.* **2018**, *2018*, 66–73. [[CrossRef](#)]
17. Costes, J.P.; Dahan, F.; Dupuis, A. Laurent, Solid state and solution studies of the compounds resulting from the equimolecular condensation of a diamine with a dione Mn monoxime. *New J. Chem.* **1997**, *21*, 1211–1217.
18. Lah, M.S.; Pecoraro, V.L. Isolation and Characterization of  $\{Mn^{II}[Mn^{III}(\text{salicylhydroximate})_4(\text{acetate})_2(\text{DMF})_6] \cdot 2\text{DMF}$ : An Inorganic Analogue of  $M^{2+}(12\text{-crown-4})$ . *J. Am. Chem. Soc.* **1989**, *111*, 7258–7259. [[CrossRef](#)]
19. Mezei, G.; Zaleski, C.M.; Pecoraro, V.L. Structural and Functional Evolution of Metallacrowns. *Chem. Rev.* **2007**, *1074*, 4933–5003. [[CrossRef](#)] [[PubMed](#)]
20. Bain, G.A.; Berry, J.F. Diamagnetic Corrections and Pascal's Constants. *J. Chem. Educ.* **2008**, *85*, 532–536. [[CrossRef](#)]
21. Costes, J.P.; Vendier, L. Cu–Ln complexes with a single  $\mu$ -oximate bridge. *C. R. Chimie* **2010**, *13*, 661–667. [[CrossRef](#)]
22. Bencini, A.; Benelli, C.; Caneschi, A.; Carlin, R.L.; Dei, A.; Gatteschi, D. Crystal and Molecular Structure of and Magnetic Coupling in Two Complexes Containing Gadolinium(III) and Copper(II) Ions. *J. Am. Chem. Soc.* **1985**, *107*, 8128–8136. [[CrossRef](#)]

23. Costes, J.P.; Dahan, F.; Dupuis, A.; Laurent, J.P. Is ferromagnetism an intrinsic property of the Cu<sup>II</sup>/Gd<sup>III</sup> couple? Part 1. Structures and magnetic properties of two novel dinuclear complexes with a  $\mu$ -phenolato- $\mu$ -oximato (Cu,Gd) core. *Inorg. Chem.* **2000**, *39*, 169–173. [[CrossRef](#)] [[PubMed](#)]
24. Costes, J.P.; Dahan, F.; Dupuis, A. Is ferromagnetism an intrinsic property of the Cu<sup>II</sup>/Gd<sup>III</sup> couple? Part 2. Structures and magnetic properties of novel trinuclear complexes with a  $\mu$ -phenolato- $\mu$ -oximato (Cu,Gd) core. *Inorg. Chem.* **2000**, *39*, 5994–6000. [[CrossRef](#)] [[PubMed](#)]
25. Boudalis, A.K.; Clemente-Juan, J.M.; Dahan, F.; Tuchagues, J.P. New Poly-Iron(II) Complexes of N<sub>4</sub>O Dinucleating Schiff Bases and Pseudohalides: Syntheses, Structures, and Magnetic and Mossbauer Properties. *Inorg. Chem.* **2004**, *43*, 1574–1586. [[CrossRef](#)] [[PubMed](#)]
26. James, F.; Roos, M. MINUIT Program, a System for Function Minimization and Analysis of the Parameters Errors and Correlations. *Comput. Phys. Commun.* **1975**, *10*, 343–367. [[CrossRef](#)]
27. Fair, C.K. *MOLLEN. An Interactive Structure Solution Procedure*; Enraf-Nonius: Delft, The Netherlands, 1990.
28. North, A.C.T.; Phillips, D.C.; Mathews, F.S. A semi-empirical method of absorption correction. *Acta Crystallogr. Sect. A* **1968**, *A24*, 351–359. [[CrossRef](#)]
29. Sheldrick, G.M. *SHELX97 [Includes SHELXS97, SHELXL97, CIFTAB]*; Programs for Crystal Structure Analysis (Release 97-2); Institut für Anorganische Chemie der Universität: Tammanstrasse 4, Göttingen, Germany, 1998.
30. Farrugia, L.J. WinGX suite for small-molecule single-crystal crystallography. *J. Appl. Crystallogr.* **1999**, *32*, 837–838. [[CrossRef](#)]
31. Ibers, J.A.; Hamilton, W.C. *International Tables for X-ray Crystallography. Vol. IV*; Kynoch Press: Birmingham, UK, 1974.
32. Dolomanov, O.V.; Bourhis, L.J.; Gildea, R.J.; Howard, J.A.K.; Puschmann, H. OLEX2: A complete structure solution, refinement and analysis program. *J. Appl. Cryst.* **2009**, *42*, 339–341. [[CrossRef](#)]



© 2018 by the authors. Licensee MDPI, Basel, Switzerland. This article is an open access article distributed under the terms and conditions of the Creative Commons Attribution (CC BY) license (<http://creativecommons.org/licenses/by/4.0/>).